Decadal oscillation of autumn precipitation in central Vietnam modulated by the East Pacific-North Pacific (EP-NP) teleconnection

R. Li[1,2], S.-Y. Wang[1,2], R.R. Gillies[1,2], B.M. Buckley[3], L.H. Truong[4], C. Cho[1,2]

(1) Utah Climate Center, Utah State University, Logan, UT, USA
(2) Department of Plants, Soils, and Climate, Utah State University, Logan, UT, USA
(3) Tree Ring Lab, Lamont-Doherty Earth Observatory of Columbia University, NY, USA
(4) Vietnam Academy of Science and Technology, SIE, HCMC, Vietnam

Email: lirong18@gmail.com

Running head: Modulation of EP-NP on fall rainfall in Vietnam

**Abstract**

Autumn precipitation over central Vietnam is associated with an increase in the occurrence of tropical cyclones that lead to frequent flooding and pose a significant threat to lives and property. The present analyses reveal a pronounced decadal oscillation of autumn precipitation in central Vietnam within the 8-11-year frequency band that is modulated by the East Pacific-North Pacific (EP-NP) teleconnection. The negative phase of the EP-NP pattern is associated with a positive sea surface temperature (SST) anomaly in the South China Sea (SCS) that induces low-level convergence, enhances convection, and increases precipitation over central Vietnam and adjacent islands including Hainan (China) and the Philippines. This circulation feature around the SCS is embedded in a large-scale circulation associated with SST anomalies across the Pacific Ocean – i.e., cooling in the eastern and central tropical Pacific sandwiched by warming in the North and South Pacific as well as the western Pacific Ocean. The positive phase of the EP-NP features opposite SST and circulation anomalies, with the result being reduced rainfall in central Vietnam. This out-of-phase relationship and shared decadal spectral coherence

between the EP-NP index and autumn precipitation in central Vietnam might be useful for future climate predictions and flood management.

**Keywords:** Decadal variability, precipitation in central Vietnam, East Pacific-North Pacific (EP-NP) pattern, teleconnection, climate change

## 1. Introduction

The country of Vietnam comprises a long, narrow stripe of mostly mountainous land along Indochina's eastern coast, spanning from the Asian tropics at roughly 23˚N to the equatorial region at about 9˚N in the Mekong Delta (Figure 1). The climate of Vietnam is regulated by different monsoonal regimes: While northern Vietnam is controlled by a summer (July, August, and September) regime, central Vietnam is unique in the Indochina Peninsula in that it is dominated by an autumnal regime with maximum precipitation occurring in autumn, coupled with an influx of tropical disturbances and cyclones [*Chen et al.,* 2012; *Nguyen et al.,* 2014]. Thus, central Vietnam's autumn (October, November, and December) precipitation frequently causes flooding that poses a significant threat to lives and properties [*Yokoi and Matsumoto,* 2008].

Most previous studies primarily researched the summer monsoon regime and tended to treat Indochina as a whole (Chen et al 1998, Chen and Yoon 2000, Hsu et al 2014, Zhang et al 2002), whereas autumn precipitation variability over central Vietnam, despite its uniqueness in the Indochina Peninsula and flood-inducing nature, has not received much attention. A recent study (Yen et al 2011) found that the principle interannual mode of autumn precipitation in central Vietnam is negatively correlated with

Sea Surface Temperature (SST) anomalies over the Niño 3.4 region. Another study (Chen et al 2012) further linked the interannual variations of central Vietnam’s autumn precipitation to SST anomalies in the western tropical Pacific. However, to our knowledge, decadal variation of autumn precipitation over central Vietnam has not been addressed. Decadal variability is of scientific importance since it is related to multi-year occurrences of flood and drought that need to be considered for climate mitigation planning and ecological impact assessments. In this paper, we present evidence that autumn precipitation across central Vietnam exhibits a strong and seemingly amplified decadal oscillation. The data used for this research are described in Section 2, and the major results of this study are presented in Section 3. A summary is provided in Section 4.

## 2. Data

We obtained monthly global precipitation data from NOAA's Precipitation Reconstruction over Land (PREC/L) (Chen et al 2002) for the period 1948–present. This dataset was based on gauge observations from over 17,000 stations collected in the Global Historical Climatology Network (GHCN) and the Climate Anomaly Monitoring System (CAMS) datasets. The PREC/L dataset was used because its mean distribution and annual cycle of precipitation agree well with those in several other gauge-based datasets (Chen et al 2002). The resolution of the precipitation dataset is $1.0° \times 1.0°$. For wind fields, we used the NCEP/NCAR Reanalysis data (Kalnay et al 1996), which has a resolution of $2.5° \times 2.5°$ and covers the time period 1948–present. The NOAA Extended Reconstructed SST V3b (Smith et al 2008, Smith and Reynolds 2004) was also used to analyze the SST forcing that drives the circulation anomalies. This global SST dataset has a resolution of 2.0° × 2.0° for the period 1854–present.

## 3. Results

The spatial distribution of Vietnam's long-term autumn precipitation (October-December) is shown in Figure 1. Maximum rainfall occurs over Vietnam's Central Highlands, with the minimum precipitation over northern Vietnam. The light blue bars in Figure 2a show the time series of the autumn precipitation anomalies averaged over the maximum precipitation region in central Vietnam (outlined in Figure 1). We conducted spectral analysis of autumn precipitation, which is shown in Figure 2b; this analysis reveals a pronounced and seemingly amplified variation with an elevated frequency band of 8-11 years. Therefore, we filtered autumn precipitation anomalies over central Vietnam within the 8-11-year frequency band, and then overlaid the filtered values in Figure 2a (black line).

Previous studies (Hsu and Chen 2011, Smith and Reynolds 2004, White and Liu 2008a, White and Liu 2008b, White and Tourre 2003) found that the largest decadal variability in the vicinity of Pacific either results from, or coexists with, an ENSO-like tropical Pacific variability. Other studies (Wang and Clark 2010a, Wang and Gillies 2013) noted that a quasi-decadal oscillation alternates climate between the eastern Pacific and the western Pacific-Indian Oceans. To explore possible teleconnection that modulates the decadal oscillation of autumn precipitation over central Vietnam, we examined the East Pacific–North Pacific (EP-NP) oscillation. The EP-NP index was developed using the Rotated Principal Component Analysis on monthly standardized height anomalies at 500 mb in the region 20°N-90°N of the Northern Hemisphere (Barnston and Livezey 1987, Bell and Janowiak 1995). The EP-NP index was obtained from the NOAA Physical Sciences Division at their website (http://www.esrl.noaa.gov/psd/). Figure 2c presents the raw and the 8-11-year bandpass filtered EP-NP index. A visual comparison with Figure 2a indicates that the filtered EP-NP and autumn precipitation anomalies are apparently out of phase; this relationship is confirmed by their correlation coefficient of -0.98. To further verify, Figure 2d shows the cross-spectrum of unfiltered precipitation anomalies with the unfiltered EP-NP index, revealing a marked coherence at the 8-11-year frequency band where the two variables are out of phase (i.e., negative values). This suggests that the decadal oscillation of autumn precipitation over central Vietnam is modulated by the EP-NP teleconnection.

To examine if similar modulation relationship exists for other places in this region, we also analyzed autumn precipitation over Hainan Island, China (Figure 1). Figures 2e-g demonstrate that autumn precipitation over Hainan Island also shows a decadal oscillation with a frequency band of 8-11 years that features an out-of-phase relationship with the EP-NP teleconnection (Figure 2c), similar to that of central Vietnam. The correlation coefficient between the filtered EP-NP and autumn precipitation anomalies over Hainan Island is remarkably high: -0.997.

To understand the mechanisms that lead to the coupled variations in the decadal frequency between autumn precipitation in central Vietnam (and Hainan Island of China) and the EP-NP index, we examined the autumn circulation and SST anomalies during the years of the strong phases of autumn EP-NP, which are defined as follows:

Strong positive autumn EP-NP:

$$EPNP \geq 1.2\,\sigma$$

and

Strong negative autumn EP-NP:

$$EPNP \ \leq -1.2\,\sigma$$

where $\sigma$ represents the standard deviation of the bandpass filtered EP-NP. Based on these criteria, we identified the years with the strongest positive autumn EP-NP values being 1958, 1959, 1967, 1968, 1976, 1977, 1985, 1986, 1994, 1995, 2004, and 2013, and those with strongest negative autumn EP-NP values being 1954, 1963, 1972, 1973, 1981, 1982, 1990, 1991, 1999, and 2000.

The composite anomalies of bandpass-filtered SST and 925 hPa streamlines during autumns with strong negative EP-NP phases are shown in Figure 3a. A positive SST anomaly appears in the South China Sea (SCS) accompanied with an anomalous low-level cyclonic circulation. Figure 3b shows the composite divergent wind anomalies superimposed with the velocity potential and precipitation anomalies during the strong negative EP-NP phases. A low-level convergence zone is centered in the SCS, coincident with the increased autumn precipitation in central Vietnam, Hainan Island, and the Philippines. On the contrary, during the positive EP-NP phases, negative SST anomalies are present in the SCS (Figure 3c), coexisting with an anomalous low-level anti-cyclonic anomaly (Figure 3c) and divergence (Figure 3d), resulting in negative precipitation anomalies over the region (Figure 3d). Also noteworthy is the center of the cyclonic/anticyclonic flows that is located right over the location of the maximum fall precipitation in central Vietnam (*cf.*, Figure 1).

To further examine the EP-NP teleconnection between Vietnam and the Pacific Ocean, Figure 4a shows the composite SST and 850hPa circulation anomalies (filtered) during the negative EP-NP phases. A distinct "ENSO-like" decadal-scale SST pattern (Zhang et al 1997) is readily visible over the Pacific Ocean, with strong cooling in the central tropical Pacific sandwiched by warming in the adjacent North and South Pacific as well as in the western Pacific Ocean. While increased trade winds are observed over much of the tropical Pacific, to the west of the Philippine Sea the wind anomalies become westerly, forming a cyclonic cell over the SCS and Indochina (Figure 4a), as revealed previously in Figures 3a,b. Of particular interest over the SCS is the diverging pattern of upper-level winds (Figure 4b), which correspond to the increased precipitation and low-level convergence there (Fig. 3b). All of these Pacific basin-wide and local-scale circulation and SST features are reversed during the positive phase of EP-NP, as shown in the composite charts of Figures 4c and 4d; this leads to reduced precipitation in central Vietnam, Hainan Island, and the Philippines (Figure 3d).

Also noteworthy is the "great-arch" pattern of a short-wave train emanating from this Southeast Asian circulation cell across the North Pacific towards western North America (along the East Asia-North Pacific rim) (Figures 4a and 4c). This wave train is equally pronounced in the 200 hPa streamlines (Figures 4b and 4d, marked by alternating H/L symbols indicating high/low pressure anomalies); this suggests a barotropic structure of the wave train across the North Pacific, in contrast to the baroclinic structure exhibited in the anomalous circulations over the SCS and Indochina. This trans-Pacific wave train is linked to the EP-NP's decadal climate modulation over the U.S. (Bumbaco et al 2013).

The next important question concerns the source of decadal variability revealed from the EP-NP pattern. Previous works (Tourre and White 1997, Zhang et al 1997) have identified marked decadal signals embedded in the ENSO indices that reveal a general El Niño/La Niña feature with a broad tropical warming/cooling band. This type of decadal variability is somewhat different from that of the Pacific Decadal Oscillation (PDO) which is limited to north of 20°N (Mantua et al 1997), even though the two patterns share a common "horseshoe" SST anomaly pattern in the North Pacific, as is evident in Figure 4. Other studies (van Loon and Meehl 2014, White and Liu 2008a) proposed that the 11-year solar cycle may play a role in driving such a pan-decadal variability in the tropics, while Wang and Clark (2010b) proposed that the feedback from ENSO-influenced tropical cyclone activity causes a 'reddening' of the climate variability signal in the central-western Pacific. However, a commonly accepted theory is lacking and the decadal signal in the EP-NP requires further research.

**4. Summary**

We analyzed precipitation variability in central Vietnam during the stormy season of autumn, and identified a significant decadal oscillation within the frequency band of 8-11 years. It was found that the decadal oscillation in the SCS and coastal Indochina is linked to the EP-NP teleconnection that affects the entire Pacific basin. During strong negative EP-NP phases, warmer SST in the SCS enhances upward motion (i.e., low-level convergence and upper-level divergence) and leads to increased rainfall over central Vietnam, Hainan Island of China, and the Philippines. These circulation anomalies are embedded in the large-scale circulation pattern between the central-eastern tropical Pacific and the western Pacific-Indian Ocean. The implication from this study is that the multi-year occurrences of flooding in central Vietnam (United Nations 2013) may be, at least partly, explained by the EP-NP teleconnection. The decadal signal, along with other signals such as the interannual signals identified by previous studies (Yen et al 2011, Chen et al 2012), may have important implications for impact assessments of climate change and disaster preparedness. This has large implications for policy decisions going forward in the face of an uncertain future climate.

**Acknowledgements**

PREC/L Precipitation data and NCEP Reanalysis data were provided by the NOAA/OAR/ESRL PSD, Boulder, Colorado, USA, from their website at http://www.esrl.noaa.gov/psd/. B.M. Buckley was supported by NSF GEO-0908971, and L.H. Truong was supported by funding from Vietnam Academy of Science and Technology.

REFERENCES

Barnston, A. and Livezey, R. 1987. Classification, Seasonality and Persistence of Low-Frequency Atmospheric Circulation Patterns. Mon. Weather Rev. **115**(6): 1083-1126.

Bell, G. and Janowiak, J. 1995. Atmospheric Circulation Associated with the Midwest Floods of 1993. Bull. Am. Meteorol. Soc. **76**(5): 681-695.

Bumbaco, K.A., Dello, K.D. and Bond, N.A. 2013. History of Pacific Northwest Heat Waves: Synoptic Pattern and Trends. J. Appl. Meteorol. Climatol. **52**(7): 1618-1631.

Chen, M., Xie, P., Janowiak, J. and Arkin, P. 2002. Global land precipitation: A 50-yr monthly analysis based on gauge observations. J. Hydrometeorol. **3**(3): 249-266.

Chen, T., Weng, S., Yamazaki, N. and Kiehne, S. 1998. Interannual variation in the tropical cyclone formation over the western North Pacific. Mon. Weather Rev. **126**(4): 1080-1090.

Chen, T. and Yoon, J. 2000. Interannual variation in Indochina summer monsoon rainfall: Possible mechanism. J. Clim. **13**(11): 1979-1986.

Chen, T., Tsay, J., Yen, M. and Matsumoto, J. 2012. Interannual Variation of the Late Fall Rainfall in Central Vietnam. J. Clim. **25**(1): 392-413.

Hsu, H. and Chen, Y. 2011. Decadal to bi-decadal rainfall variation in the western Pacific: A footprint of South Pacific decadal variability?. Geophys. Res. Lett. **38**: L03703.

Hsu, H., Zhou, T. and Matsumoto, J. 2014. East Asian, Indochina and Western North Pacific Summer Monsoon - An update. Asia-Pac. J. Atmos. Sci. **50**(1): 45-68.

Kalnay, E., Kanamitsu, M., Kistler, R., Collins, W., Deaven, D., Gandin, L., Iredell, M., Saha, S., White, G., Woollen, J., Zhu, Y., Chelliah, M., Ebisuzaki, W., Higgins, W., Janowiak, J., Mo, K.C., Ropelewski, C., Wang, J., Leetmaa, A., Reynolds, R., Jenne, R.

and Joseph, D. 1996. The NCEP/NCAR 40-year reanalysis project. Bull. Am. Meteorol. Soc. **77**(3): 437-471.

Mantua, N., Hare, S., Zhang, Y., Wallace, J. and Francis, R. 1997. A Pacific interdecadal climate oscillation with impacts on salmon production. Bull. Am. Meteorol. Soc. **78**(6): 1069-1079.

Nguyen, D., Renwick, J. and McGregor, J. 2014. Variations of surface temperature and rainfall in Vietnam from 1971 to 2010. Int. J. Climatol. **34**(1): 249-264.

Smith, T.M., Reynolds, R.W., Peterson, T.C. and Lawrimore, J. 2008. Improvements to NOAA's historical merged land-ocean surface temperature analysis (1880-2006). J. Clim. **21**(10): 2283-2296.

Smith, T. and Reynolds, R. 2004. Improved extended reconstruction of SST (1854-1997). J. Clim. **17**(12): 2466-2477.

Tourre, Y. and White, W. 1997. Evolution of the ENSO signal over the Indo-Pacific domain. J. Phys. Oceanogr. **27**(5): 683-696.

United Nations. 2013. Viet Nam: Flooding in Central Provinces, Situation Report No. 1; 20 November 2013. http://reliefweb.int/sites/reliefweb.int/files/resources/UN%20Sitrep%20No%201-%20Flooding%20in%20Central%20Provinces%20in%20November%202013%20-%20Viet%20Nam. pdf **No1**.

van Loon, H. and Meehl, G.A. 2014. Interactions between externally forced climate signals from sunspot peaks and the internally generated Pacific Decadal and North Atlantic Oscillations. Geophys. Res. Lett. **41**(1): 161-166.

Wang, S. and Clark, A.J. 2010a. NAM Model Forecasts of Warm-Season Quasi-

Stationary Frontal Environments in the Central United States. Weather Forecast. **25**(4): 1281-1292.

Wang, S. and Clark, A.J. 2010b. Quasi-decadal spectral peaks of tropical western Pacific SSTs as a precursor for tropical cyclone threat. Geophys. Res. Lett. **37**: L21810.

Wang, S. and Gillies, R.R. 2013. Influence of the Pacific quasi-decadal oscillation on the monsoon precipitation in Nepal. Clim. Dyn. **40**(1-2): 95-107.

White, W.B. and Liu, Z. 2008a. Resonant excitation of the quasi-decadal oscillation by the 11-year signal in the Sun's irradiance. J. Geophys. Res. -Oceans **113**(C1): C01002.

White, W.B. and Liu, Z. 2008b. Non-linear alignment of El Nino to the 11-yr solar cycle. Geophys. Res. Lett. **35**(19): L19607.

White, W. and Tourre, Y. 2003. Global SST/SLP waves during the 20th century. Geophys. Res. Lett. **30**(12): 1651.

Yen, M., Chen, T., Hu, H., Tzeng, R., Dinh Duc Tu, Nguyen Thi Tan Thanh and Wong, C.J. 2011. Interannual Variation of the Fall Rainfall in Central Vietnam. J. Meteorol. Soc. Jpn. **89A**: 259-270.

Yokoi, S. and Matsumoto, J. 2008. Collaborative effects of cold surge and tropical depression-type disturbance on heavy rainfall in central Vietnam. Mon. Weather Rev. **136**(9): 3275-3287.

Zhang, Y., Wallace, J. and Battisti, D. 1997. ENSO-like interdecadal variability: 1900-93. J. Clim. **10**(5): 1004-1020.

Zhang, Y., Li, T., Wang, B. and Wu, G. 2002. Onset of the summer monsoon over the Indochina Peninsula: Climatology and interannual variations. J. Clim. **15**(22): 3206-3221.

## List of Figures

Figure 1: Autumn precipitation (October-December) averaged over the period 1950-2013 from the PREC/L. The boxes delineate the areas used for precipitation time series in Figure 2 for central Vietnam and Hainan Island of China.

Figure 2: (a) The time series of autumn precipitation anomalies in central Vietnam (light blue bars), superimposed with 8-11-year filtered precipitation anomalies (black line). (b) Power spectra (thick black line) of autumn precipitation anomalies in central Vietnam, superimposed with the black dashed line representing 95% confidence level, and the red line showing Markov red noise spectrum. (c) The time series of the unfiltered autumn EP-NP index (light blue bars), superimposed with its 8-11-year filtered values (thick black line). (d) Cross spectrum between unfiltered EP-NP index and precipitation anomalies in central Vietnam; negative values indicate an out-of-phase relationship. (e), (f), and (g): Same as (a), (b), and (d) but for Hainan Island of China.

Figure 3: (a) The composite SST anomalies (color) and 925 hPa streamlines during autumns with strong negative EP-NP phases. (b) The composite divergent wind anomalies (vectors; m/s) superimposed with filtered velocity potential (lines; scaled by 1e6) and precipitation (color; mm/day) anomalies during autumns with strong negative EP-NP phases. (c) and (d): Same as (a) and (b) but for strong positive EP-NP phases.

Figure 4: (a) and (b): The composite charts of filtered SST anomalies (color) and streamlines at 850 hPa and 200 hPa during autumns with strong negative EP-NP phases. (c) and (d) : Same as Figure 4a,b but for autumns with strong positive EP-NP phases. The symbols “L” and “H” in (b) and (d) indicate the wave train with low and high pressure anomalies.

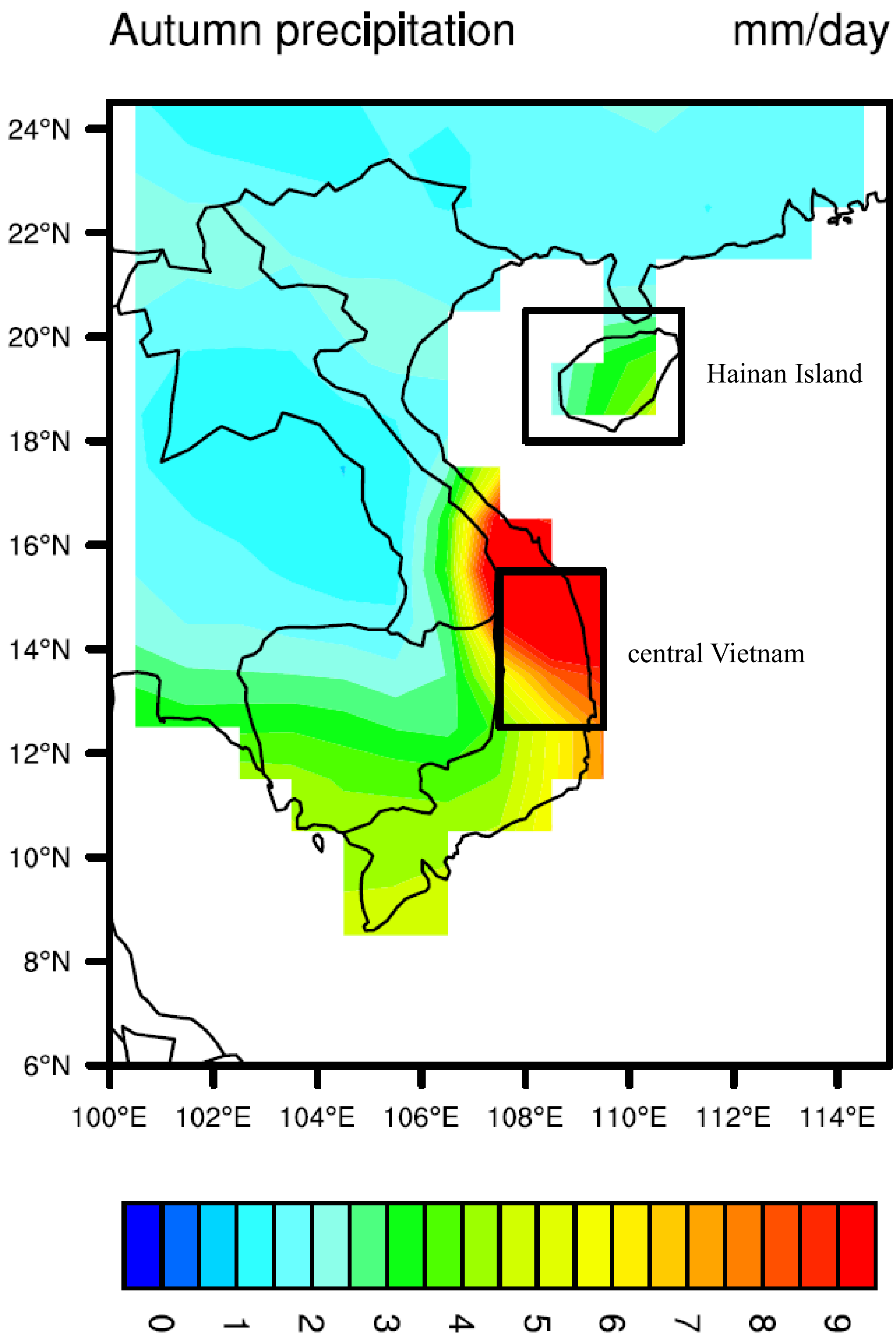


Figure 1: Autumn precipitation (October-December) averaged over the period 1950-2013 from the PREC/L. The boxes delineate the areas used for precipitation time series in Figure 2 for central Vietnam and Hainan Island of China.

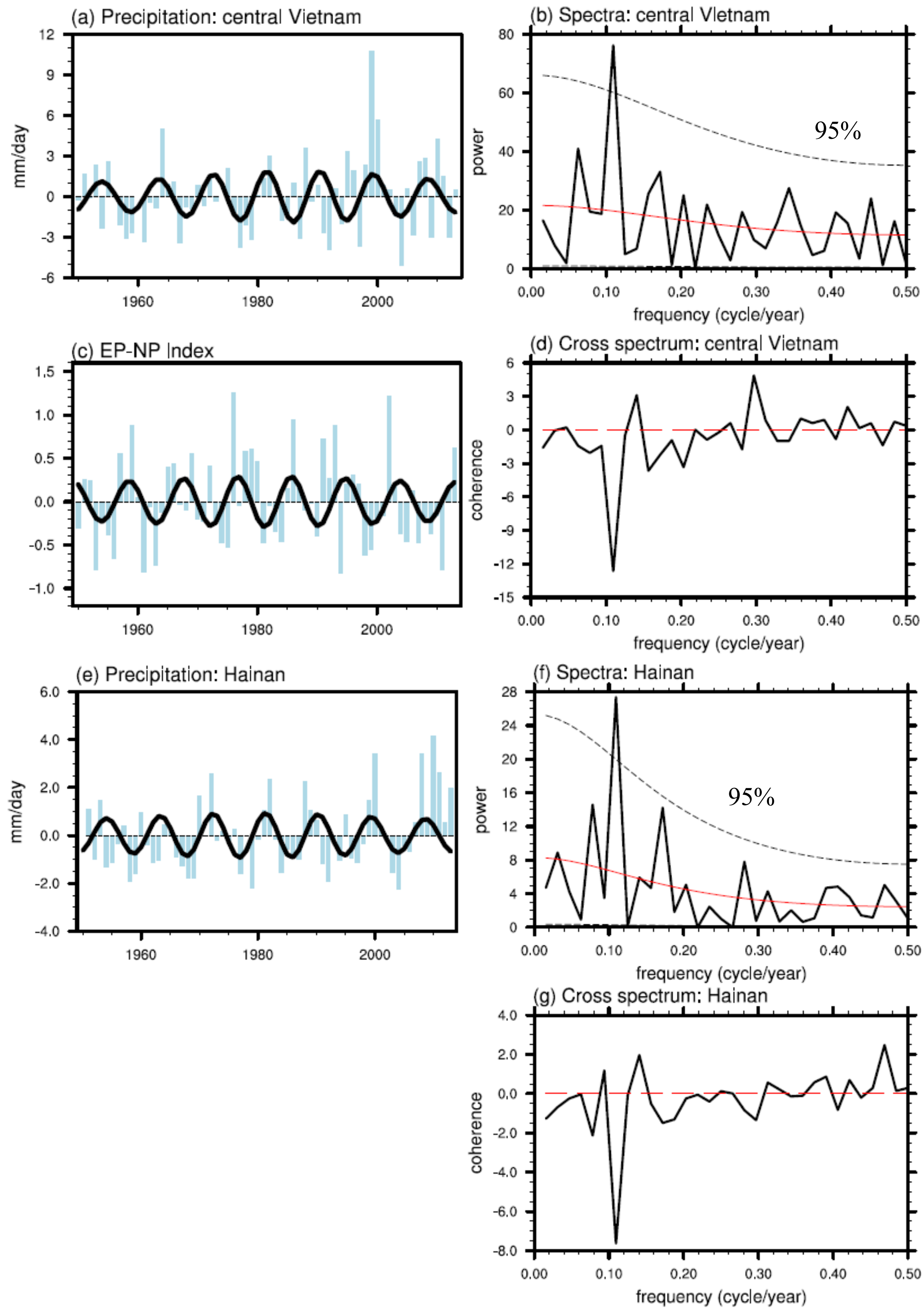


Figure 2: (a) The time series of autumn precipitation anomalies in central Vietnam (light

blue bars), superimposed with 8-11-year filtered precipitation anomalies (black line). (b) Power spectra (thick black line) of autumn precipitation anomalies in central Vietnam, superimposed with the black dashed line representing 95% confidence level, and the red line showing Markov red noise spectrum. (c) The time series of the unfiltered autumn EP-NP index (light blue bars), superimposed with its 8-11-year filtered values (thick black line). (d) Cross spectrum between unfiltered EP-NP index and precipitation anomalies in central Vietnam; negative values indicate an out-of-phase relationship. (e), (f), and (g): Same as (a), (b), and (d) but for Hainan Island of China.

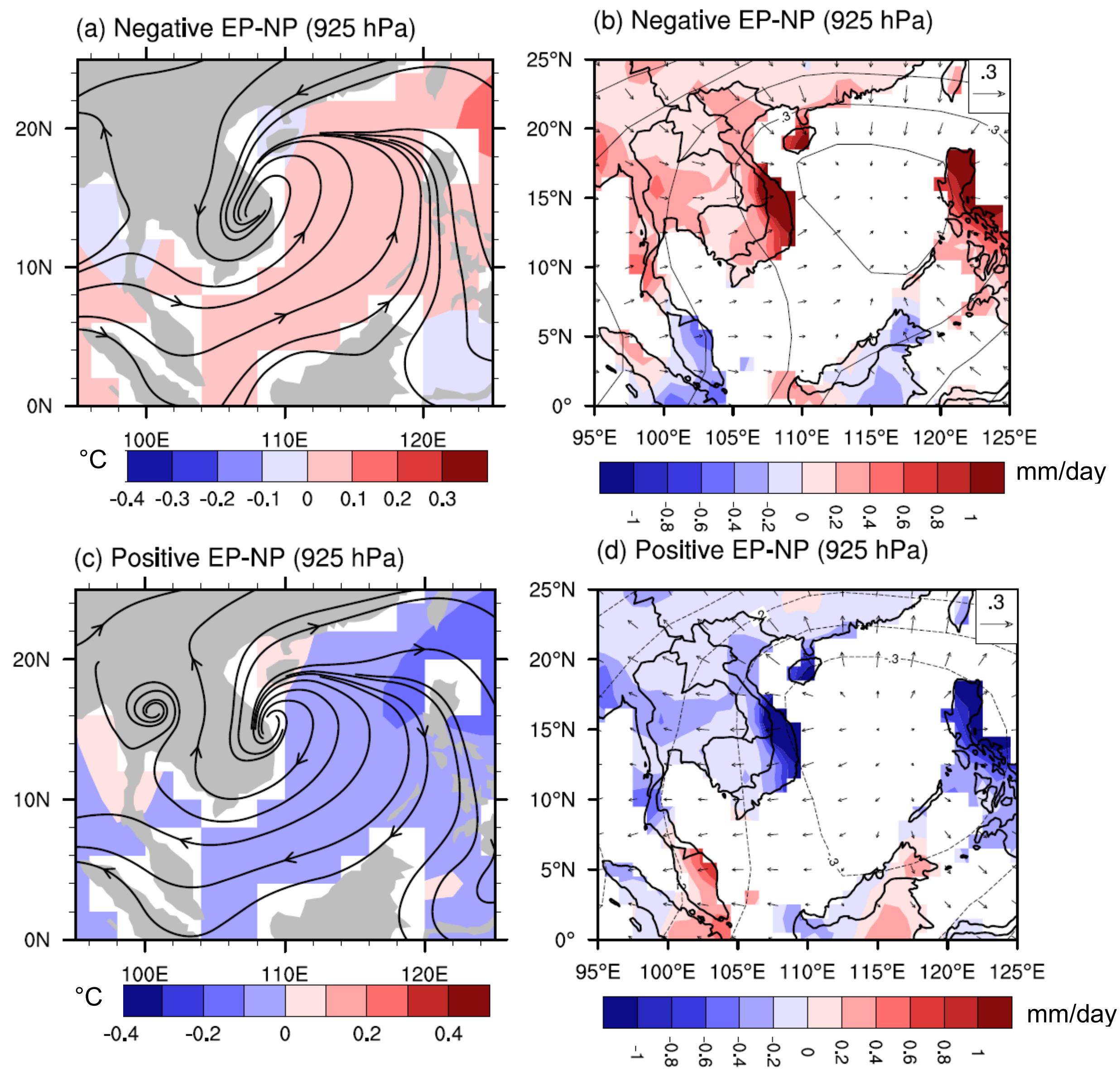


Figure 3: (a) The composite SST anomalies (color) and 925 hPa streamlines during autumns with strong negative EP-NP phases. (b) The composite divergent wind anomalies (vectors; m/s) superimposed with filtered velocity potential (lines; scaled by 1e6) and precipitation (color; mm/day) anomalies during autumns with strong negative EP-NP phases. (c) and (d): Same as (a) and (b) but for strong positive EP-NP phases.

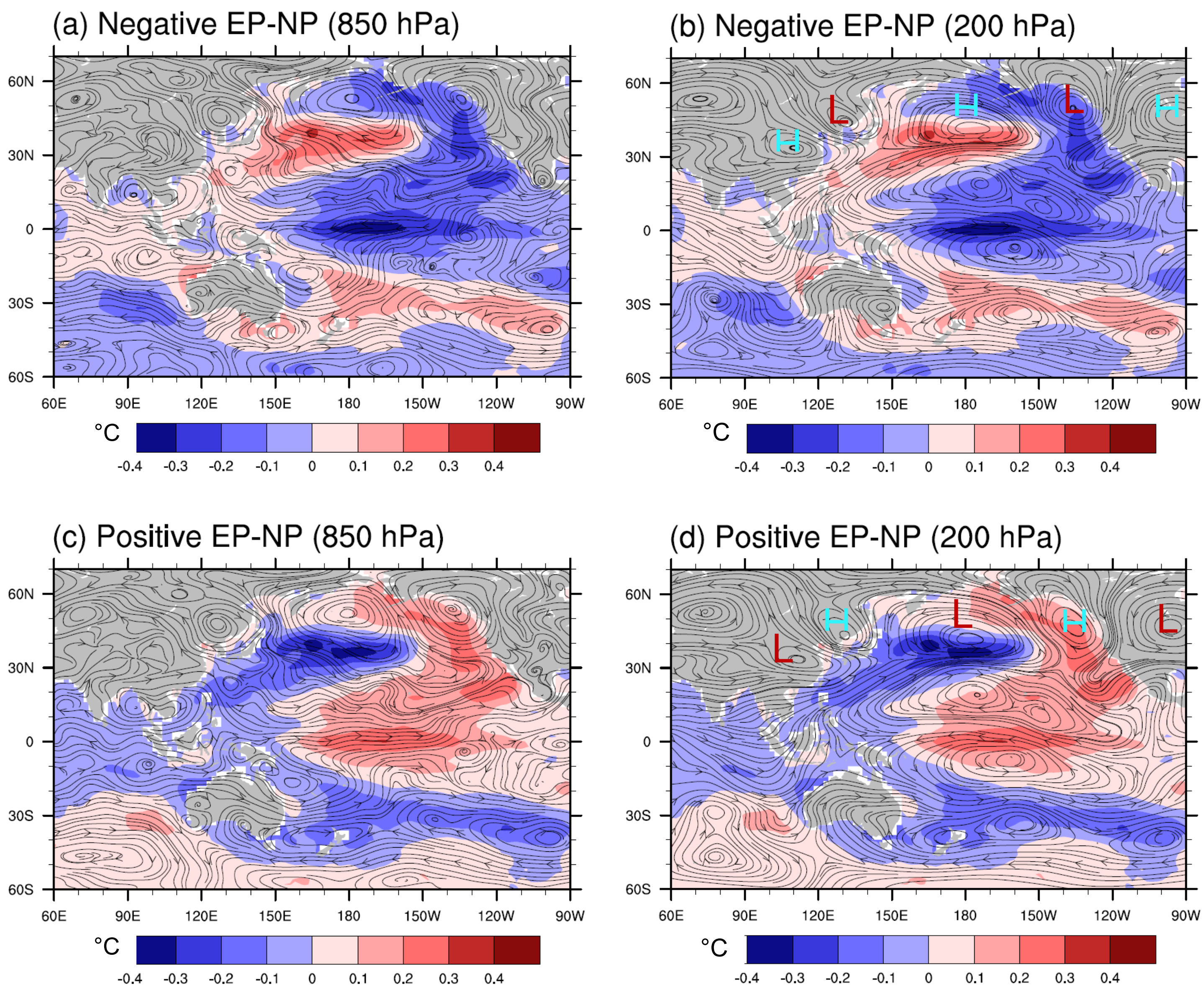


Figure 4: (a) and (b): The composite charts of filtered SST anomalies (color) and streamlines at 850 hPa and 200 hPa during autumns with strong negative EP-NP phases. (c) and (d) : Same as Figure 4a,b but for autumns with strong positive EP-NP phases. The symbols "L" and "H" in (b) and (d) indicate the wave train with low and high pressure anomalies.